Mistletoe Lectin I Is a Sialic Acid-Specific Lectin with Strict Preference to Gangliosides and Glycoproteins with Terminal Neu5Acα2−6Galβ1−4GlcNAc Residues

Johannes Müthing,*,‡ Iris Meisen,‡ Patrick Bulau,‡ Martin Langer,§ Klaus Witthohn,§ Hans Lentzen,§ Ulrich Neumann,|| and Jasna Peter-Katalinić‡

Institute for Medical Physics and Biophysics, University of Münster, Robert-Koch-Strasse 31, D-48149 Münster, Germany, VISCUM AG, D-51429 Bergisch Gladbach, Germany, and Clinic of Poultry of the Hannover School of Veterinary Medicine, D-30559 Hannover, Germany

Received August 8, 2003

ABSTRACT: Mistletoe lectin I (ML-I) is a type II ribosome-inactivating protein, which inhibits the protein biosynthesis at the ribosomal level. ML-I is composed of a catalytically active A-chain with rRNA *N*-glycosidase activity and a B-chain with carbohydrate binding specificities. Using comparative solid-phase binding assays along with electrospray ionization tandem mass spectrometry, ML-I was shown to preferentially bind to terminally α2−6-sialylated neolacto series gangliosides from human granulocytes. IV^{6}Neu5Ac-nLc4Cer, VI^{6}Neu5Ac-nLc6Cer, and VIII^{6}Neu5Ac-nLc8Cer were identified as ML-I receptors, whereas the isomeric α2−3-sialylated neolacto series gangliosides were not recognized. Only marginal binding of ML-I to terminal galactose residues of neutral glycosphingolipids with a Galβ1−4Glc or Galβ1−4GlcNAc sequence was determined, whereas a distal Galα1−4Gal, GalNAcβ1−3Gal, or GalNAcβ1−4Gal disaccharide did not bind at all. Among the glycoproteins investigated in Western blot and microwell adsorption assays, only those carrying Neu5Acα2−6Galβ1−4GlcNAc residues, exclusively, predominantly, or even as less abundant constituents in an assembly with Neu5Acα2−3Galβ1−4GlcNAc-terminated glycans, displayed high ML-I binding capacity. From our data we conclude that (i) ML-I has to be considered as a sialic acid- and not a galactose-specific lectin and (ii) neolacto series gangliosides and sialoglycoproteins with type II glycans, which share the Neu5Acα2−6Galβ1−4GlcNAc terminus, are true ML-I receptors. This strict preference might help to explain the immunostimulatory potential of ML-I toward certain leukocyte subpopulations and its therapeutic success as a cytotoxic anticancer drug.

Mistletoe lectin I (ML-I),[1] also referred to as *Viscum album* agglutinin I (VAA-I) or viscumin (terms synonymously used), is the major active constituent of mistletoe extracts increasingly used as therapeutic agents in adjuvant cancer therapy (*1*−*4*). ML-I is a heterodimeric two-chain (type II) ribosome-inactivating protein consisting of a catalytically active A-chain with rRNA *N*-glycosidase activity and a B-chain with carbohydrate binding specificity (*5*, *6*) to yet undefined receptors on the surface of target cells. In numerous studies mistletoe lectin has been reported to belong to the group of galactoside-specific/lactose-binding lectins. The enzymatic A-chain activity and the carbohydrate binding activity of the B-chain are both essential for the internalization to mediate apoptosis (*7*, *8*). ML-I elicits several types of cellular responses that may support the adjuvant effect in cancer therapy (*9*−*11*). Because of its great capacity to modulate the immune response and the potential therapeutic use of recently genetically engineered recombinant viscumin (rViscumin) as a cytostatic anticancer drug (*12*−*14*), it is important to better understand the interaction of ML-I with its carbohydrate receptors expressed on leukocytes and tumor cells.

Gangliosides, built up by a sialylated oligosaccharide chain and a ceramide moiety, are involved in cell−cell recognition and adhesion by counterpart lectins (*15*, *16*). Mammalian glycoproteins in general are decorated with N- and/or O-glycosidically linked oligosaccharide chains (*17*), which carry terminal sialic acid to various extents, a key factor for structural recognition of endogenous and pathogenic lectins (*18*).

Employing solid-phase binding assays, rViscumin has been recently shown to preferentially bind to terminally α2−6-

* Correspondence should be addressed to this author. Telephone: 49 251 83-55192. Telefax: 49 251 83-55140. E-mail: jm@uni-muenster.de.

‡ University of Münster.

§ VISCUM AG.

|| Clinic of Poultry of the Hannover School of Veterinary Medicine.

[1] Abbreviations: BCIP, 5-bromo-4-chloro-3-indolyl phosphate; BSA, bovine serum albumin; CHO, Chinese hamster ovary; CID, collision-induced dissociation; DSA, *Datura stramonium* agglutinin; EPO, erythropoietin; ESI-QTOF-MS, electrospray ionization quadrupole time-of-flight mass spectrometry; GSL(s), glycosphingolipid(s); HGG, human granulocyte gangliosides; HPLC, high-performance liquid chromatography; HPTLC, high-performance thin-layer chromatography; MAA, *Maackia amurensis* agglutinin; mab, monoclonal antibody; MALDI-TOF-MS, matrix-assisted laser desorption ionization time-of-flight mass spectrometry; ML, mistletoe lectin; ML-IA, A-chain of ML-I; ML-IB, B-chain of ML-I; Neu5Ac, *N*-acetylneuraminic acid; Neu5Gc, *N*-glycolylneuraminic acid; PBS, phosphate-buffered saline; PVP, poly(vinylpyrrolidone); SNA, *Sambucus nigra* agglutinin; TBS, Tris-buffered saline; VAA, *Viscum album* agglutinin. The designation of neutral GSLs and gangliosides follows the IUPAC−IUB recommendations (*65*).

10.1021/bi0301892 CCC: $27.50
Published on Web 02/28/2004

sialylated neolacto series gangliosides (*19*). Only marginal binding of rViscumin to galactose-terminated neutral glycosphingolipids (GSLs) was determined. In the present paper we report on novel data about the binding specificity of the native, plant-derived ML-I. Naturally occurring GSLs and serum glycoproteins of mammalian origin were used in this study to reveal a preferential binding of ML-I toward Neu5Acα2−6Galβ1−4GlcNAc epitopes shared by both lipid- and protein-bound glycans. This is the first report that clearly indicates that ML-I is to be considered rather as a sialic acid-specific than a galactose-specific type II ribosome-inactivating protein.

MATERIALS AND METHODS

ML-I and Anti-ML-IA Antibody. ML-I was isolated from an extract of mistletoe (*V. album*) by affinity chromatography on partially hydrolyzed Sepharose according to Franz et al. (*20*). ML-I working solutions were prepared from a stock solution of 1.38 mg/mL in 2.67 M ammonium sulfate by 1:100 dilution with poly(vinylpyrrolidone) (PVP) buffer [0.1 g/L PVP-10 (K12−18) in 20 mM NaH_2PO_4, 300 mM NaCl, and 1 mM EDTA, pH 8.0; Sigma, Deisenhofen, Germany], followed by final dilution with phosphate-buffered saline and 0.01% (v/v) Tween 80 (Merck-Schuchardt, Hohenbrunn, Germany; PBS−T80, pH 7.2) to the ML-I concentrations required. Bound ML-I was detected with the mouse IgG1 anti-ML-IA monoclonal antibody (mab) TA5 (*21*).

ML-I is a highly potent toxin when reaching the body via the parenteral route (intravenous, subcutaneous, and intramuscular), whereas the enteral route (oral) toxicity is relatively low. Thus, handling of this substance should be done with utmost care, using gloves and avoiding highly concentrated working solutions and sharp or pointed tools.

Reference Neutral GSLs and Gangliosides. Neutral GSL fractions contained Gb4Cer, Gb3Cer, and LacCer (erythrocytes); LacCer, nLc4Cer, nLc6Cer, and Le^x-GSLs [granulocytes (*22*); available through Alexis Corp. (Läufelfingen, Switzerland; product ID ALX-306-026-M001)]; and Gg3Cer, LacCer, and Gg4Cer [MDAY-D2 cells (*23*)]. A preparation of human brain gangliosides, composed of GM1, GD1a, GD1b, and GT1b, was purchased from Supelco Inc. (Bellefonte, PA).

Anion-Exchange HPLC Separation of Terminally α2−3- and α2−6-Sialylated Neolacto Series Gangliosides. A ganglioside mixture containing GM3, IV^3nLc4Cer, IV^6nLc4Cer, and VI^3nLc6Cer as the major constituents was isolated from human granulocytes (total human granulocyte gangliosides, HGG) as described previously (*24*). For the separation of α2−3- and α2−6-sialylated monosialogangliosides HPLC was carried out with the Superformance universal glass-cartridge device of Merck, earlier published in detail (*25*). A glass cartridge (150 mm × 10 mm) filled with Fractogel EMD TMAE-650(S) (Merck, no. 20286) was loaded with 30 mg of a GM3-depleted ganglioside mixture of human granulocytes. TMAE-Fractogel-bound gangliosides were eluted with a linear ammonium acetate gradient and collected in 1.5 mL fractions. The relative elution volume was calculated as the quotient of the elution volume to the bed volume of the column. Aliquots of single monosialoganglioside fractions were analyzed by HPTLC (*25*). Single fractions were pooled as follows: HGG1 (pool of fractions 13 and 14), HGG2 (pool of fractions 15 and 16), HGG3 (pool of fractions 24−26), and HGG4 (pool of fractions 27−29). Pooled fractions were desalted by dialysis and analyzed by HPTLC (see Results). The separation of gangliosides by thin-layer chromatography results in double bands due to the substitution of the sphingosine moiety with C24 (upper band) and C16 fatty acid (lower band) (*26*). The terminally α2−3-sialylated gangliosides IV^3nLc4Cer and VI^3nLc6Cer have been investigated by electrospray ionization quadrupole time-of-flight mass spectrometry (ESI-QTOF-MS) as recently reported (*27*). Terminally α2−6-sialylated gangliosides VI^6-nLc6Cer and $VIII^6$nLc8Cer were structurally characterized in this study by ESI-QTOF-MS.

Electrospray Ionization Quadrupole Time-of-Flight Mass Spectrometry (ESI-QTOF-MS). Gangliosides of HPLC-purified fraction HGG4 (see above) were dissolved in distilled methanol and analyzed in negative ion mode by nano-ESI-MS and low-energy collision-induced dissociation (CID) MS/MS using a quadrupole time-of-flight (QTOF) mass spectrometer (Micromass, Manchester, U.K.) equipped with a nanospray manipulator. After the precursor ion of interest was selected with the first quadrupole, CID was applied to obtain fragment ions [for further details, see Metelmann et al. (*28*)]. The nomenclature introduced by Domon and Costello (*29*) was used for the assignment of the fragment ions.

Reference Glycoproteins and Lectins. The structural features of employed glycoproteins, particularly their types of glycosylation (N- and O-glycans) and extent and mode of sialylation (α2−3- versus α2−6-linked sialic acids) together with the relevant references (*30*−*40*) are listed in Table 5.

Human plasma sialoglycoproteins transferrin, fetuin (also named α_2HS-glycoprotein), haptoglobin, and α_1-acid glycoprotein were from Calbiochem-Novabiochem GmbH (Bad Soden/Ts., Germany), and human erythropoietin (EPO, recombinant from Chinese hamster ovary cells) was from Roche Diagnostics GmbH (Mannheim, Germany). Bovine fetuin, asialofetuin, and digoxigenin-labeled *Maackia amurensis* agglutinin (MAA), *Sambucus nigra* agglutinin (SNA), and *Datura stramonium* agglutinin (DSA) were from the glycan differentiation kit (Roche Diagnostics GmbH). Bound lectins were detected with polyclonal sheep anti-digoxigenin Fab fragments conjugated with alkaline phosphatase (*41*).

Polyclonal Anti-Neu5Acα2−6Galβ1−4GlcNAc-R Antibody. A chicken was immunized with HPLC-purified IV^6-nLc4Cer according to the method of Kasai et al. (*42*). One milligram of the ganglioside was adsorbed to 1 mg of permethylated bovine serum albumin (Serva, Heidelberg, Germany) in PBS. The solution was emulsified with an equal part of Freund's adjuvant (Difco, Detroit, MI) in a final volume of 1 mL and administered at multiple intramuscular sites. Preimmune serum was taken just before immunization. After 4 weeks, the chicken was boostered and exsanguinated 14 days later.

High-Performance Thin-Layer Chromatography. GSLs were separated on silica gel-precoated glass-backed high-performance thin-layer chromatography plates (HPTLC plates, size 10 cm × 10 cm, thickness 0.2 mm; Merck, no. 5633). Neutral GSLs were chromatographed in solvent I (chloroform/methanol/water, 120/70/17, each by volume) and gangliosides in solvent II (chloroform/methanol/water, 120/

85/20, each by volume), the latter supplemented with 2 mM $CaCl_2$ (*43*). Neutral GSLs and gangliosides were visualized with orcinol.

TLC Overlay Assay. Secondary rabbit anti-chicken IgY and goat anti-mouse IgG and IgM antisera, both affinity chromatography-purified and labeled with alkaline phosphatase, were purchased from Dianova (Hamburg, Germany) and used in a 1:2000 dilution (*44*). The TLC immunostaining procedure was carried out as previously described (*45*) with some modifications.

(A) Detection of GSLs with a Polyclonal Anti-Neu5Acα2−6Galβ1−4GlcNAc-R Antibody. After thin-layer chromatography of GSLs the silica gel was fixed with polyisobutyl methacrylate (Plexigum P28; Röhm, Darmstadt, Germany) followed by incubation of the plate in PBS at 37 °C overnight. The HPTLC plate was soaked for 15 min with 1% (w/v) bovine serum albumin (BSA) in PBS (solution A1) and then overlayed for 1 h with the primary antibody diluted 1:1000 in solution A1. Terminally α2−6-sialylated neolacto series gangliosides were detected by the chicken polyclonal anti-Neu5Acα2−6Galβ1−4GlcNAc-R antibody. The plate was washed three times with 0.05% (v/v) Tween 21 in PBS (solution B) and incubated for 1 h with alkaline phosphatase-labeled rabbit anti-chicken IgY antibody diluted in solution A1. The plate was then washed three times with solvent B and once with glycine buffer (0.1 M glycine, 1 mM $ZnCl_2$, 1 mM $MgCl_2$, pH 10.4) to remove phosphate. Bound antibodies were visualized by color development of blue indigo-like stable stain after incubation with 0.05% (w/v) 5-bromo-4-chloro-3-indolyl phosphate (BCIP; Biomol, Hamburg, Germany) in glycine buffer. The overlay assay was also performed in the absence of the anti-Neu5Acα2−6Galβ1−4GlcNAc-R antibody as a control. Dye exposure times were 1.5 h.

(B) Detection of GSLs with ML-I. The ML-I binding activity toward GSLs was detected after overnight incubation of the plate in PBS at 37 °C, prewashing with PVP-buffer, followed by incubation with 1 μg/mL ML-I diluted in PVP buffer/PBS−T80 for 1 h as described above. The plate was washed three times with solution B, incubated for 15 min with solution A1, and then overlayed with the murine anti-ML-IA mab TA5 (1 μg/mL in solution A1) for 1 h. The following steps were performed as described above. Secondary alkaline phosphatase-labeled anti-mouse IgG and IgM were used for the detection of bound mouse TA5 antibody. Control overlay assays were performed (a) in the absence of ML-I and (b) using an unrelated mouse IgG1 mab (Sigma, no. N-5264, 1:500 diluted in solution A1) instead of mouse IgG1 anti-ML-IA mab TA5. Dye exposure times were 1.5 h for ML-I binding assays toward gangliosides and 20 h for ML-I binding assays toward neutral GSLs and for the controls.

Microwell Adsorption Assays. All microwell adsorption assays were carried out in duplicate on polystyrene microtiter plates (MaxiSorp F96 immuno plates; Nunc, Wiesbaden, Germany) at room temperature if not otherwise stated.

(A) Procedure for GSLs. Microwells were loaded with 10 μg (neutral GSLs from MDAY-D2 cells), 7.5 μg (neutral GSLs from human granulocytes), and 5 μg (neutral GSLs from human erythrocytes, gangliosides from human brain, and human granulocytes) of GSLs in 100 μL of methanol in serial 1:2 dilutions containing constant amounts of 50 μg of phosphatidylcholine (L-α-phosphatidylcholine; Sigma, P-0763) and 30 μg of cholesterol (5-cholesten-3β-ol; Sigma, C-8667) per well. Methanol was evaporated, and the GSL-coated microwells were provided each with 1 μg of ML-I. After 1 h incubation the wells were loaded for 1 h with the murine anti-ML-IA mab TA5 [0.8 μg/mL in 3% (w/v) BSA in PBS (solution A3)]. After incubation with alkaline phosphatase-labeled anti-mouse IgG and IgM secondary antibody diluted 1:2000 in solution A3, bound antibodies were visualized with disodium 4-nitrophenyl phosphate hexahydrate (1 mg/mL in glycine buffer). Enzyme activity was recorded after 30 min at 405 nm with an ELISA microplate reader (Model 3550; Bio-Rad, Munich, Germany).

(B) Procedure for Glycoproteins. Microwells were loaded with 0.2 μg of each glycoprotein dissolved in 100 μL of 0.1 M $NaHCO_3$ and incubated at +4 °C overnight. The wells were soaked for 2 h in 3% (w/v) BSA in Tris-buffered saline (TBS, pH 7.5) supplemented with 0.05% (v/v) Tween 20 (blocking solution). Microwells were incubated for 1.5 h in serial 1:2 dilutions of ML-I, starting with a concentration of 0.8 μg of ML-I in 100 μL of 1% (w/v) BSA in TBS−T20 and ending up with 0.0125 μg of ML-I per 100 μL. Control experiments were performed for each glycoprotein in the absence of ML-I. The wells were then loaded with anti-ML-IA monoclonal antibody TA5 [0.8 μg/mL in 1% (w/v) BSA in TBS−T20] for 1 h. Bound alkaline phosphatase-labeled anti-mouse IgG secondary antibody (1:2000 in 1% BSA in TBS−T20) was visualized, and the enzyme activity was recorded after 60 min as described above. Between each incubation step the wells were washed four times with TBS. Two additional washes with glycine buffer were performed prior to addition of the substrate solution.

SDS−PAGE. One-dimensional gel electrophoresis (*46*) was performed as SDS−PAGE under reducing conditions using 4% stacking and 12% separating gels of 0.75 mm thickness. Reference glycoproteins were fixed and stained with 0.1% Coomassie Brilliant Blue R250 in 45% methanol in 10% acetic acid for 1 h, followed by destaining with 25% methanol in 7.5% acetic acid. Standard proteins with a molecular mass range from 14 to 66 kDa were from Sigma (Deisenhofen, Germany; Dalton Mark VII-L).

Western Blot. (A) Procedure for Reference Glycoproteins. SDS−PAGE-separated glycoproteins were transferred by electroblotting onto a nitrocellulose membrane (Hybond-C extra; Amersham Life Science, Freiburg, Germany). The membrane was incubated with 3% (w/v) BSA in TBS (pH 7.5) supplemented with 0.05% (v/v) Tween 20 (TBS−T20) at +4 °C overnight, incubated with 1.0 μg/mL ML-I for 2 h, and then overlayed with anti-ML-IA mab TA5 [0.8 μg/mL in TBS−T20 with 1% (w/v) BSA] for 1.5 h. After incubation for 2 h with alkaline phosphatase-labeled anti-mouse IgG secondary antibody [1:2000 in TBS−T20 with 1% (w/v) BSA], bound antibodies were visualized with 0.05% (w/v) BCIP in TBS (pH 9.5).

(B) Procedure for ML-I. SDS−PAGE-separated ML-I was electroblotted, followed by blocking of the membrane, incubation with anti-ML-IA mab TA5, secondary antibody, and substrate solution as described above. Between each incubation step the membrane was washed four times with TBS. Two additional washes with 0.1 M Tris-HCl supplemented with 0.05 M $MgCl_2$ and 0.1 M NaCl (pH 9.5) were performed prior to addition of the substrate solution.

In-Gel Digestion of ML-I and Matrix-Assisted Laser Desorption Ionization Time-of-Flight Mass Spectrometry (MALDI-TOF-MS). In-gel digestion of SDS−PAGE-separated and Coomassie blue-stained ML-I subunits (approximately 100 pmol of protein per band) was performed by overnight incubation of the vacuum-dried gel pieces with 0.6 μg of trypsin (Roche Diagnostics GmbH, sequencing grade, no. 1418475) in 50 μL of digestion buffer at 37 °C (*47*). Peptide extracts were dried down, desalted on reversed-phase ZipTips$_{C18}$ (Millipore, Bedford, MA), evaporated to dryness, and redissolved in 4 μL of water. One microliter of the desalted peptides was mixed with an equal volume of the UV-absorbing matrix [2,5-dihydroxybenzoic acid/2-hydroxy-5-methoxybenzoic acid (9/1 w/w), 10 mg/mL in 10% ethanol], spotted onto a stainless steel target plate, and dried under a stream of air. MALDI-TOF-MS for the determination of the molecular masses of tryptic peptides was carried out in positive ion mode by use of a REFLEX TOF instrument (Bruker-Daltonik, Bremen, Germany). The experimentally derived peptide fragment masses of ML-I subunits were submitted to the SWISS-PROT database (*48*).

RESULTS

Structural Assignments to Mistletoe Lectin I (ML-I). Peptide-mass mapping is one of the most commonly employed approaches to rapidly identify proteins from a gel band or gel spot. Six micrograms of ML-I was applied to SDS−PAGE and stained with Coomassie blue. Separated ML-IA and ML-IB were in-gel-digested with trypsin, and the unfractionated peptide digests were subjected to MALDI-MS. The resulting peptide maps of ML-IA and ML-IB are shown in panels A and B of Figure 1, respectively, together with the corresponding Coomassie blue-stained bands of the ML-I subunits (inserts of Figure 1, lanes b). The experimentally derived fragment masses were submitted to the SWISS-PROT database (*49*). The peptide mass search resulted in the identification of ML-IA (rRNA *N*-glycosidase, EC 3.2.2.22) composed of 254 amino acids with a molecular mass of 28478 Da (*50*) and ML-IB composed of 264 amino acids with a molecular mass of 28981 Da (*51*), both from *V. album* (European mistletoe). The experimentally determined fragment masses and the calculated, i.e., the theoretical, masses together with the corresponding amino acid sequences are summarized in Table 1. The theoretical molecular mass of ML-IA fits well to the apparent molecular mass determined by SDS−PAGE (29 kDa; see inserts of Figure 1, lanes b). However, ML-IA carries one N-glycan at Asn^{112} with a molecular mass of 1173 Da (*50*), resulting in a total molecular mass of 29651 Da. The difference of about 5000 Da between the theorectical molecular mass of ML-IB (28981 Da) and the apparent molecular mass of 34 kDa (deduced from the SDS−PAGE) is due to the existence of three N-glycans at Asn^{61}, Asn^{96}, and Asn^{136} (*51*). The knowledge about the precise biochemical structure of the ML-I preparation used in this study is essential and the first step for the following analysis of ML-I binding characteristics toward distinct glycosphingolipids and glycoproteins.

Binding Specificity of Anti-ML-IA mab TA5. The anti-ML-IA mab TA5 binds in Western blots to the ML-I hololectin (apparent molecular mass approximately 66 kDa) after native PAGE. The antibody specifically recognizes the A-chain (ML-IA) and does not cross-react with the B-chain (ML-IB) as previously reported by Tonevitsky et al. (*21*). As a control, the Western blot of SDS−PAGE-separated ML-I with mab TA5 is shown in the insert of Figure 1A (lane c), thereby confirming the A-chain specificity of mab TA5. The purity of the preparation as a whole was assessed by SDS−PAGE before and after reduction, revealing low amounts of single A- and B-chains beside the predominant intact lectin. However, the A-chain specificity of mab TA5 and the carbohydrate binding activity of the B-chain allow fully reliable interpretation of ML-I binding assays with GSLs and glycoproteins as performed in the following paragraphs.

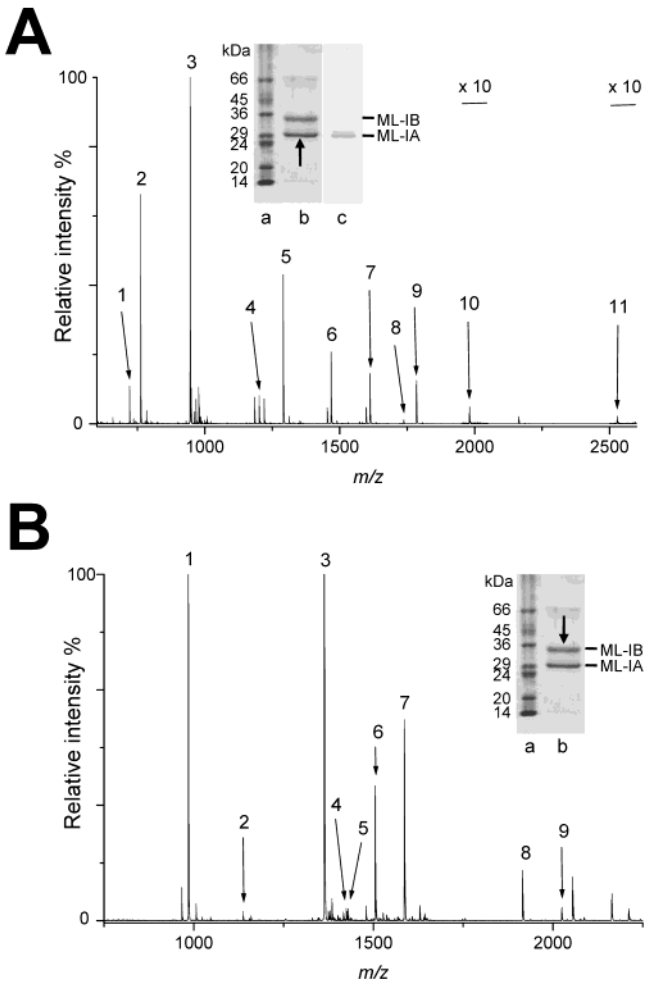

FIGURE 1: MALDI mass spectra of tryptic in-gel-digested ML-IA (A) and ML-IB (B). The inserts of panel A and panel B show the Coomassie blue-stained standard proteins (lanes a) and ML-I (lanes b, 6 μg) after SDS−PAGE under reducing conditions. The Western blot of ML-I (0.86 μg) with anti-ML-IA mab TA5 is shown in lane c of panel A. The arrows point to ML-IA or ML-IB, corresponding to the MALDI mass spectra of the A-chain and B-chain digest in panels A and B, respectively. The experimentally identified and the corresponding calculated *m*/*z* values of the molecular ions $[M + H]^+$ of the tryptic fragments are listed in Table 1.

Binding of ML-I toward Microwell Adsorbed Neutral GSLs and Gangliosides. To obtain preliminary structural information regarding GSL binding specificities of ML-I, a screening was performed using microwells coated with neutral GSL and ganglioside mixtures of well-defined structures (for structures, see Tables 2 and 3). Human erythrocytes are known to express globo series neutral GSLs Gb4Cer and Gb3Cer, the former being the dominant one. Neutral GSLs

Table 1: Experimental and Theoretical *m*/*z* Values of the Molecular Ions of In-Gel-Digested ML-IA (A) and ML-IB (B) Obtained by MALDI-MS and Their Corresponding Amino Acid Sequences[a]

peak	residue	sequence	$[M + H]^+$ *m*/*z* exptl	$[M + H]^+$ *m*/*z* calcd
		(A) Tryptic Peptides of ML-IA		
1	144−150	FPGGSTR	721.33	721.36
2	20−25	FITLLR	762.45	762.41
3	169−175	FNPILWR	945.55	945.53
4	42−52	QSTIPVSDAQR	1201.70	1201.62
5	95−106	GAETHLFTGTTR	1290.71	1290.64
6	8−19	VTHQTTGEEYFR	1467.79	1467.69
7	220−234	LAIPPGNFVTLTNVR	1612.06	1611.92
8	91−106	DAPRGAETHLFTGTTR	1730.01	1729.86
9	26−41	DYVSSGSFSNEIPLLR	1784.04	1783.87
10	126−143	DQIPLGIDQLIQSVTALR	1980.36	1980.11
11	20−41	FITLLRDYVSSGSFSNEIPLLR	2527.61	2527.36
		(B) Tryptic Peptides of ML-IB		
1	142−149	EVTIYGFR	984.55	984.52
2	104−115	SNLVLAASSGIK	1159.72	1159.67
3	175−186	WALYGDGSIRPK	1362.75	1362.72
4	42−53	SNNDPNQLWTIK	1429.75	1429.71
5	1−13	DDVTCSASEPTVR	1436.74	1436.63
6	218−230	WVFTNEGAILNLK	1504.87	1504.82
7	42−54	SNNDPNQLWTIKR	1585.89	1585.81
8	26−41	DDDFHDGNQIQLWPSK	1914.99	1914.86
9	198−217	DSVSTVINIVSCSGASGSQR	2024.15	2023.98

[a] The corresponding MALDI mass spectra of in-gel-digested ML-IA and ML-IB are shown in panels A and B of Figure 1, respectively, showing also the Coomassie blue-stained bands of ML-IA and ML-IB separated by SDS−PAGE.

of human granulocytes preferentially contain LacCer and the neolacto series GSLs nLc4Cer, nLc6Cer, and to a lower extent fucosylated derivatives of, e.g., nLc6Cer, the so-called Lewis^x GSLs. Searching for certain ganglio series neutral GSLs as potential receptors, a GSL mixture of MDAY-D2 cells was chosen due to its high content of Gg3Cer and Gg4Cer. Human brain gangliosides are suitable to investigate

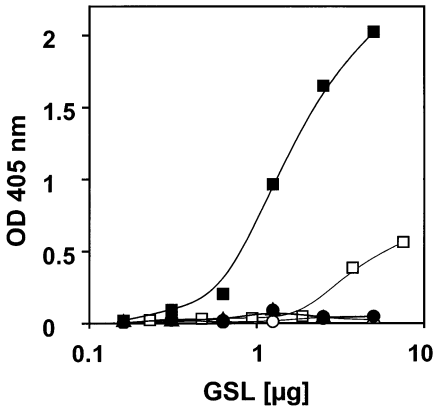

FIGURE 2: Microwell adsorption assay of neutral GSLs and gangliosides with ML-I. Microwells were loaded with GSLs in serial 1:2 dilutions and incubated with 1 μg of ML-I per well. Symbols: globo series neutral GSLs from human erythrocytes (△), neolacto series neutral GSLs from human granulocytes (□), ganglio series neutral GSLs from MDAY-D2 cells (○), human brain gangliosides (●), and human granulocyte gangliosides (■). The microwell adsorption assay reveals weak binding of ML-I toward neutral GSLs from human granulocytes and strong binding toward gangliosides from human granulocytes. The orcinol-stained thin-layer chromatogram of neutral GSLs is shown in Figure 3A and of human brain and human granulocyte gangliosides in Figure 4A. For structures, see Tables 2 and 3.

binding specificities of ganglio series gangliosides, and human granulocyte gangliosides (HGG) are the ideal candidates for exploring the binding potency of terminally α2−3- and α2−6-sialylated neolacto series monosialogangliosides.

The microwell adsorption assays of ML-I with the three reference neutral GSL preparations and the two ganglioside mixtures of well-known structures are shown in Figure 2. The only positive but rather weak reaction within the neutral GSL fractions was detected for neutral GSLs from human

Table 2: Binding of ML-I toward Neutral GSLs[a]

structure	abbreviation	ML-I[b]
Galβ1−4Glcβ1−1Cer	Lc2	(+)
Galα1−4Galβ1−4Glcβ1−1Cer	Gb3	−
GalNAcβ1−3Galα1−4Galβ1−4Glcβ1−1Cer	Gb4	−
GalNAcβ1−4Galβ1−4Glcβ1−1Cer	Gg3	−
Galβ1−3GalNAcβ1−4Galβ1−4Glcβ1−1Cer	Gg4	(+)
Galβ1−4GlcNAcβ1−3Galβ1−4Glcβ1−1Cer	nLc4	(+)
Galβ1−4GlcNAcβ1−3Galβ1−4GlcNAcβ1−3Galβ1−4Glcβ1−1Cer	nLc6	(+?)
Galβ1−4(Fucα1−3)GlcNAcβ1−3Galβ1−4GlcNAcβ1−3Galβ1−4Glcβ1−1Cer	Lewis^x	−
Galβ1−4GlcNAcβ1−3Galβ1−4GlcNAcβ1−3Galβ1−4GlcNAcβ1−3Galβ1−4Glcβ1−1Cer	nLc8	(+?)

[a] For the TLC immunostain of ML-I, see Figure 3B. [b] Appearance on immunostained TLCs graded from negative − to trace (+) positivity.

Table 3: Binding of ML-I toward Gangliosides[a]

structure	abbreviation	ML-I[b]
Neu5Acα2−3Galβ1−4Glcβ1−1Cer	GM3	−
Galβ1−3GalNAcβ1−4(Neu5Acα2−3)Galβ1−4Glcβ1−1Cer	GM1	−
Neu5Acα2−3Galβ1−3GalNAcβ1−4(Neu5Acα2−3)Galβ1−4Glcβ1−1Cer	GD1a	−
Galβ1−3GalNAcβ1−4(Neu5Acα2−8Neu5Acα2−3)Galβ1−4Glcβ-1Cer	GD1b	−
Neu5Acα2−3Galβ1−3GalNAcβ1−4(Neu5Acα2−8Neu5Acα2−3)Galβ1−4Glcβ1−1Cer	GT1b	−
Neu5Acα2−3Galβ1−4GlcNAcβ1−3Galβ1−4Glcβ1−1Cer	IV^{3}nLc4	−
Neu5Acα2−6Galβ1−4GlcNAcβ1−3Galβ1−4Glcβ1−1Cer	IV^{6}nLc4	+++++
Neu5Acα2−3Galβ1−4GlcNAcβ1−3Galβ1−4GlcNAcβ1−3Galβ1−4Glcβ1−1Cer	VI^{3}nLc6	−
Neu5Acα2−6Galβ1−4GlcNAcβ1−3Galβ1−4GlcNAcβ1−3Galβ1−4Glcβ1−1Cer	VI^{6}nLc6	+++++
Neu5Acα2−6Galβ1−4GlcNAcβ1−3Galβ1−4GlcNAcβ1−3Galβ1−4GlcNAcβ1−3Galβ1−4Glcβ1−1Cer	VIII^{6}nLc8	++++

[a] For the TLC immunostain of ML-I, see Figures 4B and 6C. [b] Appearance of immunostained TLCs graded from negative − up to highest intensity +++++.

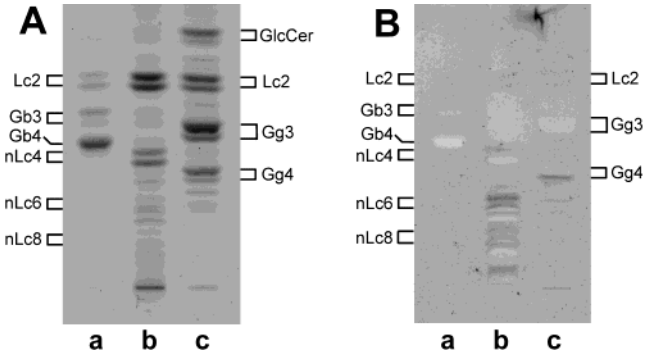

FIGURE 3: Orcinol stain (A) and ML-I TLC overlay assay (B) with globo series (a), neolacto series (b), and ganglio series neutral GSLs (c). Lanes: a, 10 μg of neutral GSLs from human erythrocytes; b, 15 μg of neutral GSLs from human granulocytes; c, 20 μg of neutral GSLs from MDAY-D2 cells. Double quantities of neutral GSLs were applied on each lane compared to the uppermost quantities used in the microwell adsorption assay in Figure 2. The TLC overlay assay reveals weak binding of ML-I toward LacCer, nLc4Cer, and Gg4Cer. Slight positive reactions at the positions of nLc6Cer and nLc8Cer cannot be structurally assigned unambiguously. For structures, see Table 2.

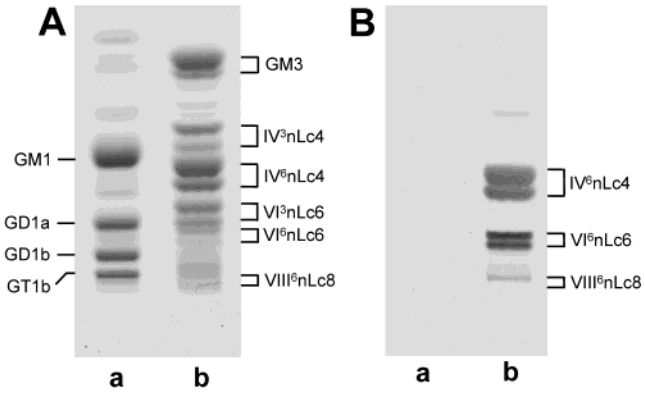

FIGURE 4: Orcinol stain (A) and ML-I TLC overlay assay (B) with ganglio series (a) and neolacto series gangliosides (b). Lanes: a, 10 μg of human brain gangliosides; b, 10 μg of HGGs. Double quantities of gangliosides were applied on each lane compared to the uppermost quantities used in the microwell adsorption assay in Figure 2. The TLC overlay assay reveals strong binding of ML-I toward α2−6-sialylated neolacto series gangliosides from human granulocytes and no binding at all toward ganglio series gangliosides from human brain. For structures, see Table 3.

granulocytes, consisting of LacCer and nLc4Cer as the main compounds. Of the two ganglioside fractions, human brain gangliosides were negative, but HGG revealed strong binding interaction with ML-I (Figure 2).

TLC Overlay Assay of Neutral GSLs with ML-I. To identify the individual neutral GSLs responsible for faint ML-I binding, TLC overlay assays were performed with neutral GSLs from human erythrocytes, human granulocytes, and murine MDAY-D2 cells. The orcinol-stained TLC of the neutral GSL fractions used is shown in Figure 3A. The TLC binding assay revealed weak positive reactions of ML-I with LacCer (Galβ1−4Glcβ1−1Cer), nLc4Cer (Galβ1−4GlcNAc terminus), and Gg4Cer (Galβ1−3GalNAc terminus) as shown in Figure 3B. Slight positive reactions of ML-I with neutral GSLs separating at positions of nLc6Cer and nLc8Cer implicate weak binding toward these structures, which are known to represent minor compounds in the neutral GSL fraction of human granulocytes. However, unambiguous structural assignments cannot be done at this stage of research. For this reason, these structures were provided with question marks in Table 2. Other neutral GSLs such as Gb3Cer, Gb4Cer, and Gg3Cer did not show any reaction. It should be mentioned that the faint binding toward neutral GSLs could only be obtained by extremely long exposure of the TLC plate for 20 h in the dye solution, thus reflecting the limit of the TLC overlay assay. Control overlay assays (a) in the absence of ML-I and (b) using an unrelated mouse IgG1 monoclonal antibody instead of mouse IgG1 anti-ML-IA mab TA5 were negative (data not shown).

TLC Overlay Assay of Gangliosides with ML-I. To identify the individual gangliosides responsible for strong ML-I binding, TLC overlay assays were performed with gangliosides from human brain and human granulocytes (HGG). A fast and clear reaction could be achieved after 1.5 h dye exposure with HGG, uncovering two strongly stained double bands (Figure 4B, lane b). Compared with the orcinol stain (Figure 4A, lane b), the gangliosides IV^{6}nLc4Cer and VI^{6}nLc6Cer can be suggested to represent the preferential receptors of ML-I. The TLC overlay assay with the human brain ganglioside fraction, containing the ganglio series

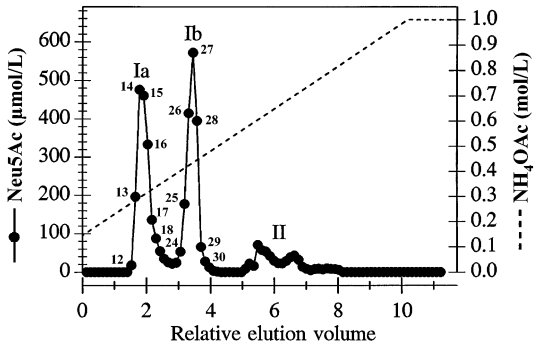

FIGURE 5: TMAE-Fractogel HPLC elution profile of a GM3-depleted ganglioside mixture from human granulocytes. Peaks: Ia, α2−3-sialylated monosialogangliosides; Ib, α2−6-sialylated monosialogangliosides; II (double peak), disialogangliosides (*25*). HGG1: pool of fractions 13 and 14. HGG2: pool of fractions 15 and 16. HGG3: pool of fractions 24−26. HGG4: pool of fractions 27−29. The orcinol-stained thin-layer chromatograms of HGG1−HGG4 are shown in Figure 6A (lanes c−f, respectively).

gangliosides GM1, GD1a, GD1b, and GT1b as shown by orcinol stain (Figure 4A, lane a), was negative and underlines the high specificity of ML-I (Figure 4B, lane a).

TLC Overlay Assays of HPLC-Separated Neolacto Series Gangliosides with Anti-IV^{6}nLc4Cer Antibody and ML-I. Figure 5 shows the preparative HPLC elution profile of a GM3-depleted HGG preparation, which resulted in two baseline-separated monosialoganglioside peaks Ia and Ib and a double-peaked disialoganglioside fraction II. Monosialoganglioside fraction Ia contains terminally α2−3-sialylated and fraction Ib terminally α2−6-sialylated neolacto-type monosialogangliosides (*25*). Single HPLC fractions were pooled as follows: fractions 13 and 14 (HGG1, containing predominantly IV^{3}nLc4Cer and minor quantities of VI^3-nLc6Cer); fractions 15 and 16 (HGG2, with the major constituent VI^{3}nLc6Cer beside minor amounts of fucosylated VI^{3}nLc6Cer); fractions 24,−26 (HGG3, comprising IV^6-nLc4Cer); fractions 27−29 (HGG4 containing IV^{6}nLc4Cer and VI^{6}nLc6Cer plus minor quantities of VIII^{6}nLc8Cer). The orcinol-stained thin-layer chromatograms of HGG1−HGG4 are shown in Figure 6A (lanes c−f, respectively) in

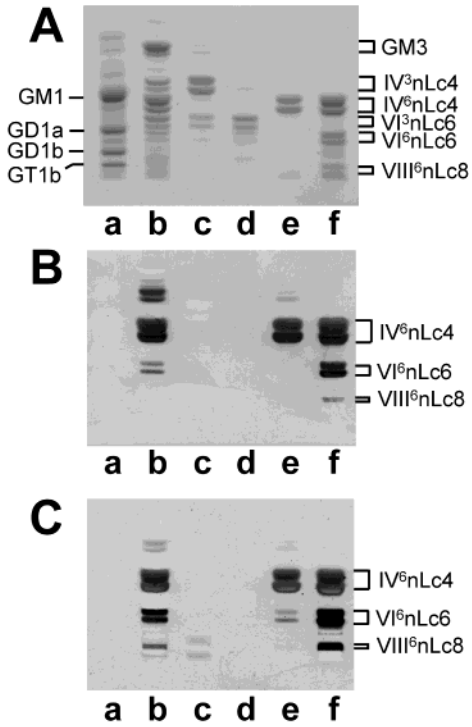

FIGURE 6: Orcinol stain (A), anti-IV^{6}nLc4Cer antibody TLC overlay assay (B), and ML-I TLC overlay assay (C) with HPLC-purified α2−3- and α2−6-sialylated neolacto series monosialogangliosides. Lanes: a, 15 μg of human brain gangliosides; b, 15 μg of human granulocyte gangliosides (HGG); c, 4 μg of IV^3-nLc4Cer (HGG1); d, 4 μg of VI^{3}nLc6Cer (HGG2); e, 4 μg of IV^6-nLc4Cer (HGG3); f, 8 μg of IV^{6}nLc4Cer, VI^{6}nLc6Cer, and VIII^{6}nLc8Cer (HGG4). Only the most prominent compounds of each HPLC fraction are mentioned. The overlay assays reveal strong and specific binding of the antibody and ML-I toward neolacto series gangliosides with terminal Neu5Acα2−6Galβ1−4GlcNAc residues and no binding at all toward neolacto series gangliosides with terminal Neu5Acα2−3Galβ1−4GlcNAc residues. For structures, see Table 3.

comparison to human brain and total human granulocyte gangliosides (lanes a and b, respectively).

As shown in Figure 6B, the anti-Neu5Acα2−6Galβ1−4GlcNAc-R antibody bound to IV^{6}nLc4Cer and VI^{6}nLc6Cer and even to trace quantities of VIII^{6}nLc8Cer in the HPLC-fractions. The isomeric structures IV^{3}nLc4Cer and VI^3-nLc6Cer (lanes c and d, respectively) were not detected. The same binding patterns were obtained in the TLC overlay binding assay with ML-I (Figure 6C), exhibiting its high specificity toward monosialogangliosides with Neu5Acα2−6Galβ1−4GlcNAc termini. Due to assaying ganglioside fractions isolated by gradient anion-exchange HPLC, any cross-reactivities to, for example, "underlying" disialogangliosides or other lipid contaminants, which are absent in the HPLC eluates Ia and Ib (*25*) but might occur in the total HGG fraction, could be excluded. Thus, the most important and unexpected result of these binding assays is the fact that with the ML-I preparation tested here and the TLC overlay assay using the neutral GSLs and gangliosides studied, greater apparent reactivities were observed with those GSLs carrying a terminal Neu5Acα2−6Galβ1−4GlcNAc sequence (see Table 3). The control overlay assay performed in the absence of the anti-Neu5Acα2−6Galβ1−4GlcNAc-R antibody was negative (not shown).

Nano-ESI-QTOF-MS/MS of α2−6-Sialylated Gangliosides. Experimental *m*/*z* values of the molecular ions of terminally α2−6-sialylated neolacto series gangliosides of fraction HGG4 obtained by ESI mass spectrometry are listed in Table 4. All ganglioside components were characterized by ceramide parts containing in general C24:1, C16:0, and (to a minor extent) C22:0 fatty acids for one core carbohydrate structure contributing to the complexity of the spectrum (not shown).

Table 4: Experimental *m*/*z* Values of the Molecular Ions of Terminally α2−6-Sialylated Neolacto Series Gangliosides of Fraction HGG4 Investigated by Nano-ESI-QTOF-MS in the Negative Ion Mode

symbol	structure	$[M - H]^-$ *m*/*z*
IV^{6}nLc4	IV^{6}Neu5Ac-nLc4Cer (d18:1/16:0)	1516.89
IV^{6}nLc4	IV^{6}Neu5Ac-nLc4Cer (d18:1/22:0)	1601.14
IV^{6}nLc4	IV^{6}Neu5Ac-nLc4Cer (d18:1/24:1)	1627.04
VI^{6}nLc6	VI^{6}Neu5Ac-nLc6Cer (d18:1/16:0)	1882.18
VI^{6}nLc6	VI^{6}Neu5Ac-nLc6Cer (d18:1/24:1)	1992.35
VIII^{6}nLc8	VIII^{6}Neu5Ac-nLc8Cer (d18:1/16:0)	2247.41
VIII^{6}nLc8	VIII^{6}Neu5Ac-nLc8Cer (d18:1/24:1)	2357.53

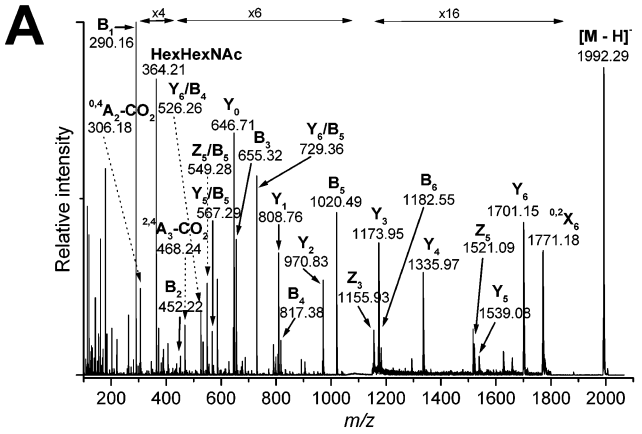

FIGURE 7: Negative ion mode nano-ESI-MS/MS spectrum (A) and fragmentation scheme with the proposed structure (B) of the ganglioside VI^{6}Neu5Ac-nLc6Cer (d18:1/24:1) with the molecular ion at *m*/*z* 1992.29 from human granulocyte ganglioside fraction HGG4.

For a detailed structural characterization of nLc6Cer and nLc8Cer species, two molecular ions (*m*/*z* 1992.35 and 2357.53; see Table 4) were selected for low-energy CID experiments. The resulting MS/MS spectra, along with the TLC immunostaining data, were consistent with their assignment as gangliosides VI^{6}Neu5Ac-nLc6Cer and VIII^6-Neu5Ac-nLc8Cer, respectively, containing C24:1 fatty acid in the ceramide portion.

A series of high-abundance Y-type ions is present in the MS/MS spectrum of the molecular ion (*m*/*z* 1992.29) of the heptasaccharide ceramide (Figure 7A), starting with loss of sialic acid (Y_6 at *m*/*z* 1701.15) and followed by consecutive cleavage of glycosidic bonds as shown in the fragmentation scheme (Figure 7B). The fragment ions are assigned according to the nomenclature for carbohydrate fragmentation of Domon and Costello (*29*). The mass differences of 162 Da

Table 5: Structural Features of Glycoproteins Used for ML-I Binding Studies in Western Blots and Microwell Adsorption Assays

lane[a]	glycoprotein	MW (kDa)[b]	N-glycans[c]	O-glycans[d]	sialylation[e]	ref
a	human transferrin	80	2 ∼85% dibranched ∼15% tribranched	0	∼5% Neu5Acα2−3-R ∼95% Neu5Acα2−6-R	*30*
b	human fetuin	48	A-chain 2 dibranched	 2 (tr)	∼40% Neu5Acα2−3-R[f] ∼60% Neu5Acα2−6-R[f]	*31*
		3	B-chain 0	 1 (tr)		
c	bovine fetuin	50	3[g] ∼15% dibranched ∼85% tribranched	3 (tr, te, he)[g]	∼55% Neu5Acα2−3-R[h] ∼45% Neu5Acα2−6-R[h]	*32*
d	bovine asialofetuin	45−50[i]	3[g] ∼15% dibranched ∼85% tribranched	3 (tr, te, he)[g]	desialylated	*33*
e	human haptoglobin	40	β-chain 4 ∼75% dibranched ∼25% tribranched	 0	<10% Neu5Acα2−3-R >90% Neu5Acα2−6-R	*34*, *35*
		17	α-chain 0	 0		
f	human α_1-acid glycoprotein	44	5 ∼10% dibranched ∼40% tribranched ∼50% tetrabranched	0	∼40% Neu5Acα2−3-R ∼60% Neu5Acα2−6-R	*36*, *37*
g	recombinant EPO	34	3 ∼2% dibranched ∼13% tribranched ∼85% tetrabranched	1 (tr, te)	≤100% Neu5Acα2−3-R[h,j] 0% Neu5Acα2−6-R	*38*−*40*

[a] According to the lanes of Figure 8 (SDS−PAGE and Western blot). [b] SDS−PAGE mobility under reducing conditions. [c] Complex-type structures. [d] Abbreviations used for O-glycans: tr = trisaccharides, te = tetrasaccharides, and he = hexasaccharides. [e] Ratio of α2−3- versus α2−6-sialylated residues. [f] Ratios determined for Neu5Ac released from total glycoprotein (N-glycans plus O-glycans). [g] Carbohydrate content: ∼80% N-glycans and ∼20% O-glycans. [h] Ratios determined for N-glycans. [i] Heterogeneous asialoglycoprotein; apparent molecular masses according to SDS−PAGE. [j] Might contain about 1−2% Neu5Gc (*40*), but both, Neu5Ac and Neu5Gc, are linked to galactose exclusively in the α2−3 configuration.

between Y_6 (*m*/*z* 1701.15) and Y_5 (*m*/*z* 1539.08) and 203 Da between Y_5 (*m*/*z* 1539.08) and Y_4 (*m*/*z* 1335.97) are typical for the loss of a hexose (e.g., galactose) and *N*-acetylhexosamine (e.g., *N*-acetylglucosamine), respectively. The sequence is completed by the Y_0 ion at *m*/*z* 646.71, representing the ceramide moiety. Confirmatory evidence for the nLc6 core-containing terminal sialic acid is provided by the full series of B-type ions from the nonreducing end of the carbohydrate chain. Additionally, a number of internal double cleavages confirmed the sequence of oligosaccharide units in the chain.

With respect to the type of sialylation (α2−3 versus α2−6 linkage of Neu5Ac), the presence of the ions $^{0,2}X_6$ (*m*/*z* 1771.18), $^{2,4}A_3 - CO_2$ (*m*/*z* 468.24), and $^{0,4}A_2 - CO_2$ (*m*/*z* 306.18), being diagnostic for α2−6-linked sialic acid (*52*), evidenced the Neu5Acα2−6Gal linkage.

In case of the low-abundance α2−6-sialylated nLc8Cer species, the structure could be elucidated by a full Y-type ion series, supported by few B-type ions. As expected, the Y-type ion series is identical to that of VI^{6}nLc6Cer up to Y_6. Due to the prolongation of the nLc8Cer chain with one HexHexNAc disaccharide, two additional Y-type ions could be detected: Y_7 at *m*/*z* 1904.22 and Y_8 at *m*/*z* 2066.55. Finally, the sequence is confirmed by a number of internal double cleavage ions and the diagnostic ions mentioned above (data not shown).

SDS−PAGE and Western Blot of Serum Glycoproteins with ML-I. In Table 5 the molecular masses, carbohydrate composition (N- and O-glycans), and type and degree of sialylation (given on a percentage level of terminal Neu5Acα2−3 and Neu5Acα2−6 linkages) of the reference glycoproteins with previously established oligosaccharide structures are summarized.

Initially, we examined the binding specificity of ML-I toward SDS-denatured glycoproteins in Western blots as shown in Figure 8. Human transferrin contains complex-type biantennary and triantennary N-glycans in ratio of ∼85:15. The two branches of the biantennary chain are generally fully α2−6-sialylated (Neu5Acα2−6Galβ1−4GlcNAc-R), while both isomeric triantennary oligosaccharides contain an additional Neu5Acα2−3Galβ1−4GlcNAc residue (*30*). The binding of ML-I toward human transferrin is shown in the Western blot of Figure 8B (lane a).

In the A-chain of human fetuin two N-glycosidic complex-type and two O-glycosidic oligosaccharides are present, while the B-chain contains only one O-glycosidically linked trisaccharide. The two biantennary N-glycans of the A-chain are almost fully α2−6-sialylated whereas the remaining three O-glycans of the protein are capped by Neu5Acα2−3 residues (*31*), resulting in an overall Neu5Acα2−6-R:Neu5Acα2−3-R ratio of 60:40. The positive binding of ML-I toward the A-chain is shown in Figure 8B (lane b).

The majority of Asn-linked oligosaccharides of bovine fetuin bear three branches (∼85%) and the remaining 15% are covered by dibranched structures (*32*). The somewhat lower content of α2−6- versus α2−3-linked Neu5Ac moieties (approximately 45% versus 55%) within both di- and tribranched structures resulted in a little lower staining intensity of ML-I toward bovine fetuin (Figure 8B, lane c) compared to, e.g., human fetuin (Figure 8B, lane b).

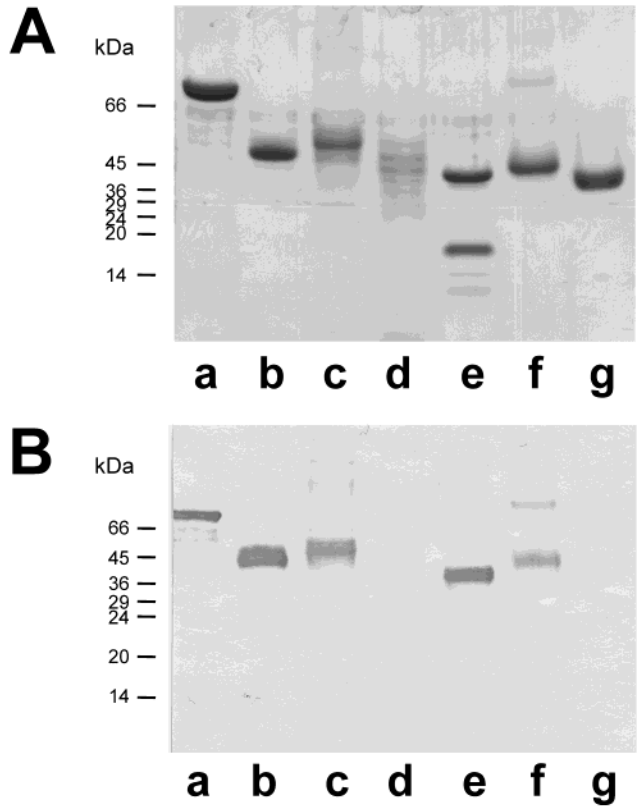

FIGURE 8: SDS−PAGE of serum glycoproteins (A) and the corresponding Western blot with ML-I (B). Protein amounts of 5 μg were applied for Coomassie blue staining and 1 μg for Western blotting. Lanes: a, human transferrin; b, human fetuin; c, bovine fetuin; d, bovine asialofetuin; e, human haptoglobin; f, human α_1-acid glycoprotein; g, recombinant (CHO cell derived) human EPO. Structural details of the glycoproteins are provided in Table 5. The Western blot reveals clear binding of ML-I toward those glycoproteins carrying N-glycans with terminal Neu5Acα2−6Galβ1−4GlcNAc residues exclusively, predominantly, or even as less abundant constituents in an assembly with Neu5Acα2−3Galβ1−4GlcNAc-terminated glycans. A very weak positive reaction was observed for asialofetuin. Recombinat EPO, carrying exclusively N-glycans with terminal Neu5Acα2−3Galβ1−4GlcNAc residues, did not show any binding.

Desialylation of bovine fetuin, however, almost completely abolished recognition by ML-I as shown in lane d of Figure 8B.

The Western blot of ML-I with human haptoglobin revealed a strong reaction with the haptoglobin β-chain (Figure 8B, lane e), similar to the stains obtained with human transferrin and human fetuin. In the β-chain, four N-glycosylation sites, predominantly (>90%) substituted by α2−6-sialylated complex-type structures, are mainly biantennary and triantennary oligosaccharides of ∼75% and ∼25%, respectively (*35*). The α-chain is not glycosylated and no binding to ML-I was detected (Figure 8B, lane e).

Human α_1-acid glycoprotein contains five N-linked chains, consisting of bi-, tri-, and tetraantennary structures in an approximate ratio of 10:40:50 (*36*) with Neu5Acα2−6 and Neu5Acα2−3 at a 6 to 4 ratio as determined by Powell and Varki (*37*). In the ML-I Western blot the binding toward human α_1-acid glycoprotein (Figure 8B, lane f), however, gave less intensive stains compared to glycoproteins possessing mostly α2−6-sialylated biantennary N-glycans, e.g., human transferrin and human fetuin.

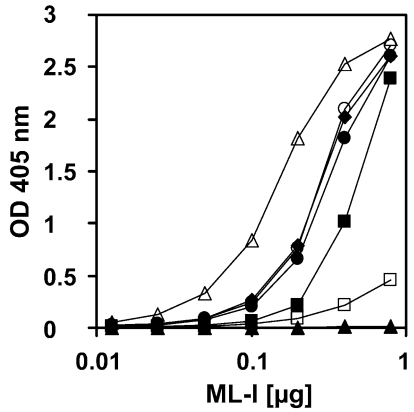

FIGURE 9: Microwell adsorption assay of serum glycoproteins with ML-I. Each microwell was loaded with 0.2 μg of glycoprotein. Microwells were incubated in serial 1:2 dilutions of ML-I, starting with 0.8 μg and ending up with 0.0125 μg of ML-I per well. Binding of ML-I to glycoproteins was detected with the anti-ML-IA mab TA5. Structural details of the glycoproteins are provided in Table 5. Symbols: human transferrin (■), human fetuin (○), bovine fetuin (◆), bovine asialofetuin (□), human haptoglobin (△), human α_1-acid glycoprotein (●), and recombinant (CHO cell derived) human erythropoietin (▲).

In the polypeptide chain of EPO one O- and three N-glycosylation sites, accounting in toto for about 40% of the molecular mass, are known. The N-linked oligosaccharides of recombinant human EPO produced in CHO cells consist of biantennary (∼2%), triantennary (∼13%), and tetraantennary complex-type chains (∼85%). All of these glycans are α2−3-sialylated, whereas those of the human urinary EPO express both Neu5Acα2−6 and Neu5Acα2−3 (*39*). ML-I does not recognize CHO cell-derived EPO at all, as shown in the Western blot (Figure 8B, lane g).

In a series of control experiments with digoxigenin-labeled lectins with defined carbohydrate specificities, strong binding of DSA (specific for Galβ1−4GlcNAc-R) to asialofetuin was recorded as proof for the presence of desialylated complex-type structures, representing only weak ligands for ML-I. MAA, specific for galactose with a terminal Neu5Acα2−3 linkage, recognized recombinant EPO (which was negative for ML-I), and SNA confirmed the Neu5Acα2−6Galβ1−4GlcNAc specificity of ML-I due to its reaction with the same sialoglycoproteins (data not shown).

Microwell Adsorption Assays of Native Serum Glycoproteins with ML-I. To investigate the influence of the epitope presentation upon ML-I binding, i.e., recognition of oligosaccharides either presented on denatured glycoproteins (membrane-fixed glycoproteins after SDS−PAGE under reducing conditions) or exposed on the native species (adsorbed to the surface of microtiter plates), the same set of glycoproteins was used for microwell adsorption assays. To reveal some quantitative comparison, immobilized glycoproteins (0.2 μg per well) were incubated with decreasing concentrations (1:2 dilutions) of ML-I, starting with 0.8 μg and ending up with 0.0125 μg per well. Different but concentration-dependent binding curves of ML-I toward the glycoproteins used were obtained (Figure 9). As shown for recombinant EPO, ML-I has no detectable interaction with oligosaccharides containing α2−3-linked sialic acid residues. On the other hand, strong positive reactions are observed for glycoproteins predominantly carrying α2−6-sialylated structures, such as human haptoglobin and human fetuin. The

positive reaction of ML-I toward bovine fetuin was strongly diminished after desialylation, indicated by the lowered steepness of the binding curve of asialofetuin. Thus, these data correlate well with and confirm the Western blot assays.

DISCUSSION

The first step in the biological action of ML-I is recognition and binding of specific ligands on the surface of target cells. When glycoproteins serve as a source for presentation of glycoligands, the individual contribution of each epitope is difficult to discern. After desialylation of human α_1-acid glycoprotein and fetuin these substrates were less prone to precipitate with ML-I (*53*), and the inhibition of the glycoprotein−lectin interaction by Neu5Acα2−3/α2−6Galβ1−4Glc was taken as evidence that ML-I is specific for sialic acid.

The initial approach using the TLC overlay technique provided the key information that neolacto series gangliosides containing a Neu5Acα2−6Galβ1−4GlcNAc epitope at the nonreducing terminus are targets for ML-I-mediated adhesion. This novel and surprising result was found to be the important prerequisite for the correct interpretation of the ensuing Western blot analyses of serum glycoproteins. Among the glycoproteins investigated, those carrying Neu5Acα2−6Galβ1−4GlcNAc residues, exclusively, predominantly, or even as less abundant constituents in an assembly with Neu5Acα2−3Galβ1−4GlcNAc-terminated glycans, displayed a high ML-I binding potency, thereby confirming the novelty that ML-I is not a galactoside-specific lectin. However, it would be required for future experiments to perform quantitative binding studies with the defined glycosphingolipids to compare their kinetic binding characteristics to ML-I. In this regard it would be important to ascertain the monomer/aggregate state of the ML-I prior to binding. This could have important implications in the interpretation of specificity of binding; i.e., ML-I aggregates and monomers may show different binding characteristics toward sialylated and nonsialylated compounds.

Recent reinvestigation of ricin adhesion specificity demonstrated that this lectin is a galactose-specific lectin expressing preference for Galβ1−4GlcNAc disaccharides (*19*). On the other hand, rViscumin from *Escherichia coli* showed preferential binding to terminally α2−6- compared to α2−3-sialylated neolacto series gangliosides (*19*), the same specificity as found for ML-I and shown in the present report. Due to the absence of ST6Gal-I CHO cells do not express lipid- or protein-bound glycans with Neu5Acα2−6Galβ1−4GlcNAc residues on their cell surface, resulting in resistance toward rViscumin cytotoxicity (*19*). In this context, the uptake of ML-I and ricin into 3T3 cells has been recently shown by Moisenovich et al. (*54*) to occur via different receptors and endocytotic pathways. Their cytological data reflect the biological proof of the predicted different types of receptors, being in excellent agreement with our structural data concerning the binding specificity of ML-I as shown in the present paper.

The carbohydrate moieties of ML-I have been characterized in detail by NMR spectroscopy in conjunction with sugar analysis by Debray et al. (*55*) and further investigated by mass spectrometric analysis by Stoeva et al. (*56*). A xylomannose-type oligosaccharide structure ($Man_3Xyl_1Fuc_1$-$GlcNAc_2$) was found to be linked to Asn^{112} of the A-chain. The same oligosaccharide is linked to Asn^{61} of the B-chain. Asn^{96} as well as Asn^{136} of the B-chain carries $Man_6GlcNAc_2$ oligosaccharides. Due to oligosaccharide microheterogeneity of mistletoe lectins from different harvest batches, Asn^{136} might also carry oligosaccharide $Man_5GlcNAc_2$. Concerning the possible influence of the N-glycans on the binding reactivity of ML-I, the activities of nonglycoslyated rViscumin (*E. coli*) and glycosylated ML-I have been compared by Eck et al. (*13*). Cytotoxicity was determined using MOLT-4 cells, and enzymatic rRNA *N*-glycosidase activity was measured in a coupled transcription/translation assay. The IC_{50} values of the two lectins were similar in both assays. Using lactose as a competitor 50% competition of binding to asialofetuin was achieved at 1.6 mM (rViscumin) and 1.8 mM (ML-I). Thus, using three different assays, no siginificant differences between the nonglycosylated recombinant protein and glycosylated ML-I could be detected (*13*), indicating the strong coincidence of biological activity and binding specificity previously explored for rViscumin (*19*) and described for ML-I in this report.

Following cell surface binding of ML-I and ensuing signaling, several cellular responses such as secretion of cytokines, namely, tumor necrosis factor-α, interleukin-1, and interleukin-6 by human peripheral blood mononuclear cells, can be measured in the nontoxic dose range in vitro and in vivo (*1*, *9*, *57*, *58*). Studies on animals and humans proved that ML-I causes significant increase and activation of natural killer cells and enhances phagocytotic activity of granulocytes and monocytes (*2*). The question, which type of oligosaccharides, i.e., protein- and/or lipid-bound, is recognized by ML-I and elicits the numerous immunoresponses, remains unanswered at this stage of research. Accumulated expression of Neu5Acα2−6Galβ1−4GlcNAc epitopes on hematopoietic cells might explain the specific action of ML-I and rViscumin as immune stimulants, i.e., to trigger the release of cytokines when applied in low concentrations.

Unlike ricin, ML-I-containing extracts are medically applied in adjuvant therapy for the treatment of human cancer, and rViscumin is now in several phase I clinical trials in Europe (*14*). Cancer cells are often characterized by the presence of "tumor-associated" GSL antigens (*59*), and some have been found to be overexpressed on certain tumor cells. Increased α2−6 sialylation of N-glycans and accumulation of gangliosides with Neu5Acα2−6Galβ1−4GlcNAc structures have been reported for hepatocellular carcinoma (*60*, *61*). Furthermore, elevated α2−6 sialyltransferase activities have been detected in several types of tumors, e.g., human colorectal cancer tissues and human choriocarcinoma (*62*, *63*), and a high degree of ST6Gal-I expression in human breast tumors was found to be an indicator of a poor prognosis (*64*).

Clinical application of low concentrations of ML-I and rViscumin induces a cellular stress response that triggers the release of cytokines by acting as immune stimulants. At high concentrations both operate as potent cytotoxins inducing apoptosis in tumor cells. In the present study clear evidence is provided that neolacto series gangliosides and complex-type N-glycans with Neu5Acα2−6Galβ1−4GlcNAc epitopes might be responsible for the immunomodulatory potency and/or tumor cell targeting of ML-I.

ACKNOWLEDGMENT

Dr. Johannes Müthing dedicates this paper to his father, Otto Müthing, who passed away while this work was in progress. The expert technical assistance of Mr. Ewald Kalthoff is gratefully acknowledged. We thank Prof. Dr. Franz Hillenkamp for access to the MALDI-TOF mass spectrometer.

REFERENCES

1. Hajto, T., Hostanska, K., Frei, K., Rordorf, C., and Gabius, H.-J. (1990) Increased secretion of tumor necrosis factor α, interleukin 1, and interleukin 6 by human mononuclear cells exposed to *β*-galactoside-specific lectin from clinically applied mistletoe extract, *Cancer Res. 50*, 3322−3326.
2. Beuth, J. (1997) Clinical relevance of immunoactive mistletoe lectin-I, *Anti-Cancer Drugs 8*, S53−S55.
3. Stauder, H., and Kreuser, E.-D. (2002) Mistletoe extracts standardised in terms of mistletoe lectins (ML I) in oncology: current state of clinical research, *Onkologie 25*, 374−380.
4. Mengs, U., Gothel, D., and Leng-Peschlow, E. (2002) Mistletoe extracts standardized to mistletoe lectins in oncology: review on current status of preclinical research, *Anticancer Res. 22*, 1399−1407.
5. Barbieri, L., Battelli, M. G., and Stirpe, F. (1993) Ribosome-inactivating proteins from plants, *Biochim. Biophys. Acta 1154*, 237−282.
6. Eschenburg, S., Krauspenhaar, R., Mikhailov, A., Stoeva, S., Betzel, C., and Voelter, W. (1998) Primary structure and molecular modeling of mistletoe lectin I from Viscum album, *Biochem. Biophys. Res. Commun. 247*, 367−372.
7. Lavastre, V., Pelletier, M., Saller, R., Hostanska, K., and Girard, D. (2002) Mechanisms involved in spontaneous and Viscum album agglutinin-I-induced human neutrophil apoptosis: Viscum album agglutinin-I accelerates the loss of antiapoptotic Mcl-1 expression and the degradation of cytoskeletal paxillin and vimentin proteins via caspase, *J. Immunol. 168*, 1419−1427.
8. Langer, M., Möckel, B., Eck, J., Zinke, H., and Lentzen, H. (1999) Site-specific mutagenesis of mistletoe lectin: The role of RIP activity in apoptosis, *Biochem. Biophys. Res. Commun. 264*, 944−948.
9. Möckel, B., Schwarz, T., Zinke, H., Eck, J., Langer, M., and Lentzen, H. (1997) Effects of mistletoe lectin I on human blood cell lines and peripheral blood cells: cytotoxicity, apoptosis and induction of cytokines, *Drug Res. 47*, 1145−1151.
10. Bantel, H., Engels, I. H., Voelter, W., Schulze-Osthoff, K., and Wesselborg, S. (1999) Mistletoe lectin activates caspase-8/FLICE independently of death receptor signaling and enhances anticancer drug-induced apoptosis, *Cancer Res. 59*, 2083−2090.
11. Savoie, A., Lavastre, V., Pelletier, M., Hajto, T., Hostanska, K., and Girad, D. (2000) Activation of human neutrophils by the plant lectin Viscum album agglutinin-I: modulation of de novo protein synthesis and evidence that caspases are involved in induction of apoptosis, *J. Leukocyte Biol. 68*, 845−853.
12. Eck, J., Langer, M., Möckel, B., Baur, A., Rothe, M., Zinke, H., and Lentzen, H. (1999) Cloning of the mistletoe lectin gene and characterization of the recombinant A-chain, *Eur. J. Biochem. 264*, 775−784.
13. Eck, J., Langer, M., Möckel, B., Witthohn, K., Zinke, H., and Lentzen, H. (1999) Characterization of recombinant and plant-derived mistletoe lectin and their B-chain, *Eur. J. Biochem. 265*, 788−797.
14. Habeck, M. (2003) Mistletoe compound enters clinical trials, *Drug Discov. Today 8*, 52−53.
15. Müthing, J. (2001) Mammalian glycosphingolipids, in *Glycoscience: Chemistry and Chemical Biology. Vol. 3: Glycolipids* (Freiser-Reid, B., Tatsuka, K., and Thiem, J., Eds.) pp 2220−2249, Springer-Verlag, Heidelberg, Germany.
16. Hakomori, S.-I. (2002) The glycosynapse, *Proc. Natl. Acad. Sci. U.S.A. 99*, 225−232.
17. Paulson, J. C. (1989) Glycoproteins: what are the sugar chains for?, *Trends Biochem. Sci. 14*, 272−276.
18. Sharon, N. (1993) Lectin-carbohydrate complexes of plants and animals: an atomic view, *Trends Biochem. Sci. 18*, 221−226.
19. Müthing, J., Burg, M., Möckel, B., Langer, M., Metelmann-Strupat, W., Werner, A., Neumann, U., Peter-Katalinić, J., and Eck, J. (2002) Preferential binding of the anticancer drug rViscumin (recombinant mistletoe lectin) to terminally α2−6-sialylated neolacto-series gangliosides, *Glycobiology 12*, 485−497.
20. Franz, H., Ziska, P., and Kindt, A. (1981) Isolation and properties of three lectins from mistletoe (Viscum album L.), *Biochem. J. 195*, 481−484.
21. Tonevitsky, A. G., Rakhmanova, V. A., Agapov, I. I., Shamshiev, A. T., Usacheva, E. A., Prokoph'ev, S. A., Denisenko, O. N., Alekseev, Y., and Pfüller, U. (1995) The interactions of anti-MLI monoclonal antibodies with isoform of the lectin from Viscum album, *Immunol. Lett. 44*, 31−34.
22. Müthing, J., and Kemminer, S. E. (1996) Nondestructive detection of neutral glycosphingolipids with lipophilic anionic fluorochromes and their employment for preparative high-performance thin-layer chromatography, *Anal. Biochem. 238*, 195−202.
23. Müthing, J., and Čačić, M. (1997) Glycosphingolipid expression in human skeletal and heart muscle assessed by immunostaining thin-layer chromatography, *Glycoconjugate J. 14*, 19−28.
24. Müthing, J., Spanbroek, R., Peter-Katalinić, J., Hanisch, F.-G., Hanski, C., Hasegawa, A., Unland, F., Lehmann, J., Tschesche, H., and Egge, H. (1996) Isolation and structural characterization of fucosylated gangliosides with linear poly-N-acetyllactosaminyl chains from human granulocytes, *Glycobiology 6*, 147−156.
25. Müthing, J. (2000) High-performance liquid chromatography of glycosphingolipids, *Methods Enzymol. 312*, 45−64.
26. Müthing, J., Unland, F., Heitmann, D., Orlich, M., Hanisch, F.-G., Peter-Katalinić, J., Knäuper, V., Tschesche, H., Kelm, S., Schauer, R., and Lehmann, J. (1993) Different binding capacities of influenza A and Sendai viruses to gangliosides from human granulocytes, *Glycoconjugate J. 10*, 120−126.
27. Metelmann, W., Müthing, J., and Peter-Katalinić, J. (2000) Nano-electrospray ionization quadrupole time-of-flight tandem mass spectrometry analysis of a ganglioside mixture from human granulocytes, *Rapid Commun. Mass Spectrom. 14*, 543−550.
28. Metelmann, W., Peter-Katalinić, J., and Müthing, J. (2001) Gangliosides from human granulocytes: a nano-ESI QTOF mass spectrometry fucosylation study of low abundance species in complex mixtures, *J. Am. Soc. Mass Spectrom. 12*, 964−973.
29. Domon, B., and Costello, C. E. (1988) A systematic nomenclature for carbohydrate fragmentations in FAB-MS/MS spectra of glycoconjugates, *Glycoconjugate J. 5*, 397−409.
30. Spik, G., Debruyne, V., Montreuil, J., van Halbeek, H., and Vliegenthart, J. F. G. (1985) Primary structure of two sialylated triantennary glycans from human serotransferrin, *FEBS Lett. 183*, 65−69.
31. Watzlawick, H., Walsh, M. T., Yoshioka, Y., Schmid, K., and Brossmer, R. (1992) Structure of the N- and O-glycans of the A-chain of human plasma α_2HS-glycoprotein as deduced from the chemical compositions of the derivatives prepared by stepwise degradation with exoglycosidases, *Biochemistry 31*, 12198−12203.
32. Green, E. D., Adelt, G., Baenziger, J. U., Wilson, S., and van Halbeek, H. (1988) The asparagine-linked oligosaccharides on bovine fetuin, *J. Biol. Chem. 263*, 18253−18268.
33. Yet, M.-G., Chin, C. C. Q., and Wold, F. (1988) The covalent structure of individual N-linked glycopeptides from ovomucoid and asialofetuin, *J. Biol. Chem. 263*, 111−117.
34. Kurosky, A., Barnett, D. R., Lee, T.-H., Touchstone, B., Hay, R. E., Arnott, M. S., Bowman, B. H., and Fitch, W. M. (1980) Covalent structure of human haptoglobin: a serine protease homolog, *Proc. Natl. Acad. Sci. U.S.A. 77*, 3388−3392.
35. Ferens-Sieczkowska, M., and Olczak, M. (2001) Carbohydrate structures of haptoglobin in sera of healthy people and a patient with congenital disorder of glycosylation, *Z. Naturforsch. 56c*, 122−131.
36. Yoshima, H., Matsumoto, A., Mizuochi, T., Kawasaki, T., and Kobata, A. (1981) Comparative study of the carbohydrate moieties of rat and human plasma α_1-acid glycoprotein, *J. Biol. Chem. 256*, 8476−8484.
37. Powell, L. D., and Varki, A. (1994) The oligosaccharide binding specificities of CD22*β*, a sialic acid-specific lectin of B cells, *J. Biol. Chem. 269*, 10628−10636.
38. Sasaki, H., Bothner, B., Dell, A., and Fukuda, M. (1987) Carbohydrate structures of erythropoietin expressed in Chinese hamster ovary cells by a human erythropoietin cDNA, *J. Biol. Chem. 262*, 12059−12076.
39. Takeuchi, M., Takasaki, S., Miyazaki, H., Kato, T., Hoshi, S., Kochibe, N., and Kobata, A. (1988) Comparative study of the asparagine-linked sugar chains of human erythropoietins purified

from urine and the culture medium of recombinant Chinese hamster ovary cells, *J. Biol. Chem. 263*, 3657−3663.
40. Hokke, C. H., Bergwerff, A. A., van Dedem, G. W. K., Kamerling, J. P., and Vliegenthart, J. F. G. (1995) Structural analysis of the sialylated N-and O-linked carbohydrate chains of recombinant human erythropoietin expressed in Chinese hamster ovary cells, *Eur. J. Biochem. 228*, 981−1008.
41. Haselbeck, A., Schickaneder, E., von der Eltz, H., and Hösel, W. (1990) Structural characterization of glycoprotein carbohydrate chains by using digoxigenin-labeled lectins on blots, *Anal. Biochem. 191*, 25−30.
42. Kasai, M., Iwamori, M., Nagai, Y., Okumura, K., and Tada, T. (1980) A glycolipid on the surface of mouse natural killer cells, *Eur. J. Immunol. 10*, 175−180.
43. Müthing, J. (2002) TLC and HPLC of glycosphingolipids, in *Carbohydrate Analysis by Modern Chromatography and Electrophoresis* (El Rassi, Z., Ed.) Journal of Chromatography Library, Vol. 66, Chapter 13, pp 423−482, Elsevier, Amsterdam, The Netherlands.
44. Duvar, S., Peter-Katalinić, J., Hanisch, F.-G., and Müthing, J. (1997) Isolation and structural characterization of glycosphingolipids of in vitro propagated bovine aortic endothelial cells, *Glycobiology 7*, 1099−1109.
45. Müthing, J. (1998) TLC in structure and recognition studies of glycosphingolipids, in *Methods in Molecular Biology, Vol. 76: Glycoanalysis Protocols* (Hounsell, E. F., Ed.) pp 183−195, Humana Press, Totowa, NJ.
46. Laemmli, U. K. (1970) Cleavage of structural proteins during the assembly of the head of bacteriophage T4, *Nature 227*, 680−685.
47. Shevchenko, A., Wilm, M., Vorm, O., and Mann, M. (1996) Mass spectrometric sequencing of proteins from silver-stained polyacrylamide gels, *Anal. Chem. 68*, 850−858.
48. Patterson, S. D., and Aebersold, R. (1995) Mass spectrometric approaches for the identification of gel-separated proteins, *Electrophoresis 16*, 1791−1814.
49. Bairoch, A., and Apweiler, R. (2000) The SWISS-PROT protein sequence database and its supplement TrEMBL in 2000, *Nucleic Acid Res. 28*, 45−48.
50. Soler, M. H., Stoeva, S., Schwamborn, C., Wilhelm, S., Stiefel, T., and Voelter, W. (1996) Complete amino acid sequence of the A chain of mistletoe lectin I, *FEBS Lett. 399*, 153−157.
51. Soler, M. H., Stoeva, S., and Voelter, W. (1998) Complete amino acid sequence of the B chain of mistletoe lectin I, *Biochem. Biophys. Res. Commun. 246*, 596−601.
52. Meisen, I., Peter-Katalinić, J., and Müthing, J. (2003) Discrimination of neolacto-series gangliosides with α2−3- and α2−6-linked N-acetylneuraminic acid by nanoelectrospray ionization low-energy collision-induced dissociation tandem quadrupole TOF MS, *Anal. Chem. 75*, 5719−5725.
53. Wu, A. M., Song, S.-C., Hwang, P.-Y., Wu, J. H., and Pfüller, U. (1995) Interaction of mistletoe toxic lectin-I with sialoglycoproteins, *Biochem. Biophys. Res. Commun. 214*, 396−402.
54. Moisenovich, M., Tonevitsky, A., Agapov, I., Niwa, H., Schewe, H., and Bereiter-Hahn, J. (2002) Differences in endocytosis and intracellular sorting of ricin and viscumin in 3T3 cells, *Eur. J. Cell Biol. 81*, 529−538.
55. Debray, H., Wieruszeski, J. M., Strecker, G., and Franz, H. (1992) Structural analysis of the carbohydrate chains isolated from mistletoe (Viscum album) lectin I, *Carbohydr. Res. 236*, 135−143.
56. Stoeva, S., Maier, T., Soler, M. H., and Voelter, W. (1999) Carbohydrate chains and their binding sites in mistletoe lectin I, *Pol. J. Chem. 73*, 125−133.
57. Stein, G. M., Henn, W., von Laue, H. B., and Berg, P. A. (1998) Modulation of the cellular and humoral immune responses of tumor patients by mistletoe therapy, *Eur. J. Med. Res. 3*, 194−202.
58. Ribéreau-Gayon, G., Jung, M. L., Frantz, M., and Anton, R. (1997) Modulation of cytotoxicity and enhancement of cytokine release induced by Viscum album L. extracts or mistletoe lectins, *Anti-Cancer Drugs 8*, S3−S8.
59. Hakomori, S.-I. (1998) Cancer-associated glycosphingolipid antigens: their structure, organization, and function, *Acta Anat. 161*, 79−90.
60. Pousset, D., Piller, V., Bureaud, N., Monsigny, M., and Piller, F. (1997) Increased α2,6 sialylation of N-glycans in a transgenic mouse model of hepatocellular carcinoma, *Cancer Res. 57*, 4249−4256.
61. Taki, T., Yamamoto, K., Takamatsu, M., Ishii, K., Myoga, A., Sekiguchi, K., Ikeda, I., Kurata, K., Nakayama, J., Handa, S., and Matsumoto, M. (1990) Accumulation of gangliosides with N-acetylneuraminosyl(α2−6)lactosamine structure in primary human hepatoma, *Cancer Res. 50*, 1284−1290.
62. Dall'Olio, F., Malagolini, N., Di Stefano, G., Minni, F., Marrano, D., and Serafini-Cessi, F. (1989) Increased CMP-NeuAc:Galβ1,-4GlcNAc-R α2,6 sialyltransferase activity in human colorectal cancer tissues, *Int. J. Cancer 44*, 434−439.
63. Fukushima, K., Hara-Kuge, S., Seko, A., Ikehara, Y., and Yamashita, K. (1998) Elevation of α2→6 sialyltransferase and α1→2 fucosyltransferase activities in human choriocarcinoma, *Cancer Res. 58*, 4301−4306.
64. Recchi, M.-A., Hebbar, M., Hornez, L., Harduin-Lepers, A., Peyrat, J.-P., and Delannoy, P. (1998) Multiple reverse transcription polymerase chain reaction assessment of sialyltransferase expression in human breast cancer, *Cancer Res. 58*, 4066−4070.
65. Chester, M. A. (1998) Nomenclature of lipids, *Eur. J. Biochem. 257*, 293−298.

BI0301892